*Acta of Bioengineering and Biomechanics*
*Vol. 18, No. 3, 2016*

Original paper
DOI: 10.5277/ABB-00244-2014-03

# Simulations of thermal processes in tooth proceeding during cold pulp vitality testing

MARIUSZ CIESIELSKI[1]*, BOHDAN MOCHNACKI[2], JAROSŁAW SIEDLECKI[3]

[1] Institute of Computer and Information Sciences, Częstochowa University of Technology, Częstochowa, Poland.
[2] Higher School of Labour Safety Management, Katowice, Poland.
[3] Institute of Mathematics, Częstochowa University of Technology, Częstochowa, Poland.

*Purpose*: This paper deals with the mathematical modeling of the thermal processes occurring in the tooth, during a very brief contact (a few seconds) with a very cold liquid on a part of the tooth crown. In this way one can simulate a heat transfer in tooth proceeding during a dental diagnostic test – pulp vitality testing. The impact of rapid ambient thermal changes acting on the tooth can cause toothache. *Methods*: The mathematical model: a system of partial differential equations with initial-boundary conditions (the axially-symmetrical problem) and their numerical solutions using the control volume method is discussed. *Results***:** Simulation results of the kinetics of the temperature changes inside the tooth are presented. The example of the control volume mesh (using the Voronoi polygons) well describing the shape of a molar tooth is given. *Conclusions*: The simulation results (the temperature distribution in the tooth at any moment of the simulation time and the kinetics of temperature variation at the points of the tooth domain considered) can help dentists in the selection of an appropriate method of treatment.

*Key words*: *bio-heat transfer, mathematical modeling, thermal processes, tooth tissue, dental pulp testing*

## 1. Introduction

Dental pulp testing (also known as a vitality test or a sensibility testing) [1], [2], [7], [8] is an investigation that provides important diagnostic information to the dental clinician. The tooth is composed of three layers: enamel, dentil and the pulp. The outer layer, the enamel, is made of hard crystal and is the most inorganic one. The dentin lies just under the enamel and is the main structure of the tooth having properties as a bone-like substance. The dentine consists of microscopic fluid-filled channels called dentine tubules. In the middle of the tooth is the pulp. The "healthy" pulp is the vital tissue consisting of numerous blood vessels, nerves and cells, but the pulp in the traumatized tooth is not necessarily innervated.

There are two general types of pulp testing [1], [7]: a thermal test (cold and heat) and an electrical one. In this paper, only cold thermal test is considered. In this test, a refrigerant (i.e., dichlorodifluoromethane, ethyl chloride at –50 °C) is sprayed on a small cotton pellet and applied to the tooth crown. This test causes contraction of the dentinal fluid within the dentinal tubules. The rapid flow of fluid in these tubules results from the hydrodynamic forces acting on the nerve fibers. This can cause a sharp sensation (pain) in the healthy, innervated pulp of the tooth, which takes a few seconds after the removal of cold stimulus [2].

The research presented in this paper is related to the computations of temperature distribution in the molar tooth. The aim of this paper is the mathematical modeling of the thermal processes occurring in the tooth tissues (enamel, dentin, pulp) being in contact with cold liquid (a moistened cotton pellet). Different contact times with the cold liquid are analyzed. The geometry of the tooth is treated here as an axially-

* Corresponding author: Mariusz Ciesielski, Institute of Computer and Information Sciences, Częstochowa University of Technology, ul. Dąbrowskiego 73, 42-200 Częstochowa, Poland. Tel: +48 34 3250589, e-mail: mariusz.ciesielski@icis.pcz.pl
Received: November 28th, 2014
Accepted for publication: September 21st, 2016

symmetrical domain. The detailed knowledge of thermal processes occurring in the tooth domain will allow optimization of diagnostics and treatment strategies for clinical applications. There is a need to study the thermal behavior of tooth, and it is the main aim of this research.

The heat transfer in the tooth domain was considered, e.g., in work [18], but the mathematical model is based on the Fourier equation. In works [5], [19], simulations were considered that related to different types of dental fillings in a tooth which was in contact with a cold liquid. The research in paper [10] deals with the thermal stimulation (the 1D task) of dentine correlated with fluid flow in the dentinal tubule. It should be pointed out that the pulp is a vital tissue, and the models based on the Pennes equation containing terms with the blood perfusion and metabolism should be applied. Details concerning the bioheat transfer models can be found, among others, in [4], [10], [12]–[14]. It is evident that the analytical solution of the problem considered is impossible and the numerical methods should be used. In this paper, the control volume method (CVM) [3], [6] using the Voronoi tessellation [16] in order to construct the geometrical mesh covering the tooth domain is applied.

The choice of the numerical method is not accidental. The CVM (in particular using the Voronoi tessellation) constitutes a very effective tool for an approximate solution of boundary-initial problems connected with the mathematical models of heat transfer processes. The different shapes of control volumes allow us to reconstruct the real shape of the 2D object both in the case of the homogeneous and heterogeneous domain. The domain discretization can be locally concentrated, for example, close to the external boundary. The shape of Voronoi polygons offers us the possibility of correct and exact recording energy balances formulation. They constitute the base for construction of the final system of linear equations corresponding to the transition from time $t$ to time $t + \Delta t$.

# 2. Materials and methods

## 2.1. Mathematical model

The tooth domain (treated as the axially symmetrical object) is shown in Fig. 1. The domain consists of the following sub-domains: the enamel ($\Omega_1$), the dentin ($\Omega_2$) and the pulp ($\Omega_3$). The outer surface limiting the domain (boundaries $\Gamma_{b1}$ and $\Gamma_{b2}$) is in thermal contact with environment (air). Additionally, in a short period of time, the boundary $\Gamma_{b2}$ is subjected to the very cold liquid. The boundary $\Gamma_0$ represents contact with the gum.

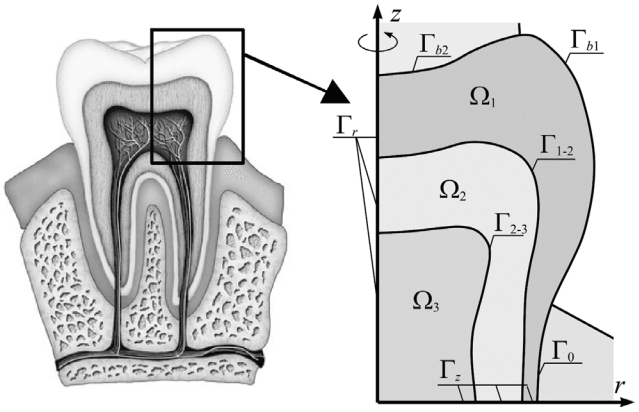


Fig. 1. Structure of a typical molar tooth [source: http://www.polskistomatolog.pl] and the tooth domain considered (longitudinal section)

The temperature field in the domain considered is described by the following system of equations

$$c_m(T)\frac{\partial T_m(r,z,t)}{\partial t} = \nabla\cdot[\lambda_m(T)\nabla T_m(r,z,t)] + Q_{per\,m}(T) + Q_{met\,m}(T), \quad m = 1,2,3, \tag{1}$$

where index $m$ identifies the particular sub-domains (1 – the enamel, 2 – the dentin, 3 – the pulp), $T$ [°C] is the temperature, $r$, $z$ [m], $t$ [s] denote spatial coordinates and time, $c$ [J/(m$^3$ °C)], $\lambda$ [W/(m °C)] are the volumetric specific heat and the thermal conductivity, respectively. The Laplace operator in the cylindrical axisymmetrical coordinates system is given as

$$\nabla\cdot[\lambda_m(T)\nabla T_m(r,z,t)] = \frac{1}{r}\frac{\partial}{\partial r}\left(r\lambda_m(T)\frac{\partial T_m(r,z,t)}{\partial r}\right) + \frac{\partial}{\partial z}\left(\lambda_m(T)\frac{\partial T_m(r,z,t)}{\partial z}\right). \tag{2}$$

In equation (1), the terms $Q_{per}$ and $Q_{met}$ [W/m$^3$] are the capacities of volumetric internal heat sources connected with the blood perfusion and metabolism, respectively. Assuming that the pulp is fed by a large number of uniformly spaced capillary blood vessels and the blood vessels are not present in the dentil and enamel, one has

$$Q_{per\,m}(T)=\begin{cases}0, & \text{if } m=1,2,\\ c_b G_{b3}(T)[T_b-T_3(r,z,t)], & \text{if } m=3,\end{cases} \quad (3)$$

where $G_{b3}$ is the blood perfusion rate in the pulp [$m^3_{(blood)}$/(s $m^3_{(tissue)}$)], $c_b$ is the blood volumetric specific heat, and $T_b$ is the blood temperature. The metabolic heat source $Q_{met\,3}$ in the pulp sub-domain can be treated as a constant value or a temperature-dependent function [10], and simultaneously $Q_{met\,1} = Q_{met\,2} = 0$ for the enamel and dentil sub-domains have been assumed.

Equation (1) is supplemented by the boundary-initial conditions. For $t = 0$ the initial condition is known

$$T_m(r,z,t)\,|_{t=0}=T_{init}, \quad m=1,2,3. \quad (4)$$

On the contact surfaces between tooth sub-domains, the continuity conditions are assumed

$$(r,z)\in\Gamma_{k-l}:\begin{cases}-\lambda_k\dfrac{\partial T_k(r,z,t)}{\partial n}=-\lambda_l\dfrac{\partial T_l(r,z,t)}{\partial n}\\ T_k(r,z,t)=T_l(r,z,t)\end{cases} \quad (5)$$

$$(k,l)\in\{(1,2),(2,3)\},$$

where $\partial/\partial n$ is a normal derivative. On the external surfaces of the sub-domains, the Dirichlet (on the surfaces – $\Gamma_0$ and $\Gamma_z$) and the Robin (on the surface of the tooth crown – $\Gamma_{b1}$ and $\Gamma_{b2}$) boundary conditions are given

$$(r,z)\in\{\Gamma_0,\Gamma_z\}:\ T_m(r,z,t)=T_{tissue}, \quad m=1,2,3, \quad (6)$$

$$(r,z)\in\Gamma_{b1}:-\lambda_1\frac{\partial T_1(r,z,t)}{\partial n}$$

$$=\alpha_{air}[T_1(r,z,t)-T_{amb\,air}(t)], \quad (7)$$

$$(r,z)\in\Gamma_{b2}:-\lambda_1\frac{\partial T_1(r,z,t)}{\partial n}$$

$$=\begin{cases}\alpha_{air}[T_1(r,z,t)-T_{amb\,air}(t)]\\ \quad \text{for } t\in(0,t_1]\cup(t_1+t_{contact},t_2]\\ \alpha_{liq}[T_1(r,z,t)-T_{amb\,liq}(t)]\\ \quad \text{for } t\in(t_1,t_1+t_{contact}]\end{cases} \quad (8)$$

where $\alpha_{air}$, $\alpha_{liq}$ [W/($m^2$ °C)] are the convective heat transfer coefficients and $T_{amb\,air}$, $T_{amb\,liq}$ [°C] are the temperatures of the air or fluid, respectively. In the mathematical model the following simplifications are assumed: the temperature of the fluid grows according to a given function and the heat transfer coefficients are treated as the constant values (dependent on several factors (fluid velocity, surface geometry, nature of motion, etc.). Time $t_1$ is a moment of simulation time at which the contact of the moistened cotton pellet with cold liquid takes place. Time $t_{contact}$ is the contact time of the pellet with the tooth crown and $t_2$ is the final time of simulation. In the time interval $t \in (0, t_1]$, the patient has an open mouth and breathing – this causes cooling of the tooth with respect to the initial temperature before starting a diagnostic test. On the boundary $\Gamma_r$, the non-flux boundary condition is given

$$(r,z)\in\Gamma_r:\left.\frac{\partial T_m(r,z,t)}{\partial r}\right|_{r=0}=0, \quad m=1,2,3. \quad (9)$$

## 2.2. Control volume method

At the stage of numerical modeling the control volume method (CVM) using the Voronoi tessellation has been used. A similar version of CVM for the 2D task was discussed in detail by Ciesielski and Mochnacki in [3], [6]. In this paper, the control volumes are in the shape of rings. So, the domain analyzed (the longitudinal section) of the tooth is divided into $N$ volumes (the section of the ring-shaped element corresponds to the shape of the Voronoi polygon). In Fig. 2, the example of the control volume mesh ($N$ = 1835) and the selected control volume are presented.

The CVM algorithm allows one to find the transient temperature field at the set of nodes corresponding to the central points of the control volumes, while the nodal temperatures are found on the basis of energy balances for the successive CV.

In Fig. 3, the cross-section of control volume $CV_i$ with the central node $p_i = (r_i, z_i)$ is presented. This cross-section is a non-regular $n_i$-sided polygon, at the same time $n_i$ is the number of adjacent control volumes $CV_{i(j)}$, for $j$ = 1, ..., $n_i$, containing the nodes $p_{i(j)}$. Subscript $i(j)$ indicates the index number of the adjacent CV. The distance between nodes $p_i$ and $p_{i(j)}$ is denoted by $h_{i(j)}$, whereas the area of contact surface (here, the surface obtained by rotation of the polygon side around the $z$ axis) between two adjacent $CV_i$ and $CV_{i(j)}$ is equal to $A_{i(j)}$ and the volume of ring-shaped $CV_i$ is denoted by $\Delta V_i$. If the polygon surface $A_{i(j)}$ is covered by the outside boundary of sub-domains then the "virtual" neighbouring node $p_{i(j)}$ lies outside the domain considered and in the computational algorithm,

the index $i(j)$ represents the index (tag) of the boundary (here, $\Gamma_0$, $\Gamma_{b1}$, $\Gamma_{b2}$, $\Gamma_r$ or $\Gamma_z$).

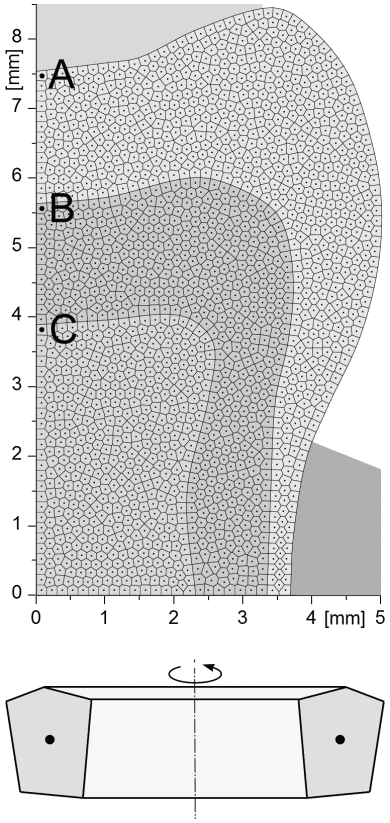


Fig. 2. The control volume mesh in the section of the tooth and selected ring-shaped control volume

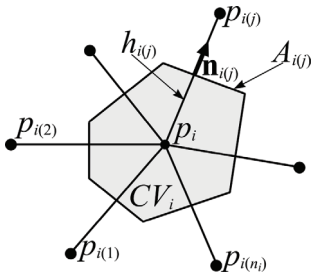


Fig. 3. Control volume $CV_i$

It is assumed for each control volume $CV_i$ that the thermal capacities and the capacities of internal heat sources are concentrated at the nodes representing elements, while the thermal resistances are concentrated on the sectors joining the nodes. The energy balances corresponding to the heat exchange between the analyzed control volume $CV_i$ and adjoining control volumes result from the integration of energy equation (1) with respect to time $t$ and volume $CV_i$. Let us consider the interval of time $\Delta t = t^{f+1} - t^f$. Then,

$$\int_{t^f}^{t^{f+1}} \int_{CV_i} c_m(T) \frac{\partial T_m(r,z,t)}{\partial t} \mathrm{d}V\mathrm{d}t$$
$$= \int_{t^f}^{t^{f+1}} \int_{CV_i} \nabla \cdot [\lambda_m(T) \nabla T_m(r,z,t)] \mathrm{d}V\mathrm{d}t$$
$$+ \int_{t^f}^{t^{f+1}} \int_{CV_i} [Q_{per\,m}(T) + Q_{met\,m}(T)] \mathrm{d}V\mathrm{d}t. \qquad (10)$$

Applying the divergence theorem for the volume $CV_i$ bounded by the surface $A_i = \bigcup_{j=1}^{n_i} A_{i(j)}$ one obtains

$$\int_{t^f}^{t^{f+1}} \int_{CV_i} c_m(T) \frac{\partial T_m(r,z,t)}{\partial t} \mathrm{d}V\mathrm{d}t$$
$$= \int_{t^f}^{t^{f+1}} \int_{A_i} \mathbf{n} \cdot [\lambda_m(T) \nabla T_m(r,z,t)] \mathrm{d}A\mathrm{d}t$$
$$+ \int_{t^f}^{t^{f+1}} \int_{CV_i} [Q_{per\,m}(T) + Q_{met\,m}(T)] \mathrm{d}V\mathrm{d}t. \qquad (11)$$

The numerical approximation of the left-hand side of equation (11) can be accepted in the form

$$\int_{t^f}^{t^{f+1}} \int_{CV_i} c_m(T) \frac{\partial T_m(r,z,t)}{\partial t} \mathrm{d}V\mathrm{d}t$$
$$\cong c_i^f (T_i^{f+1} - T_i^f) \Delta V_i \qquad (12)$$

where $c_i^f$ is an integral mean of thermal capacity and this value is approximated by the volumetric specific heat corresponding to the temperature $T^f$ (explicit scheme). The source term in equation (11) for the pulp sub-domain $\Omega_3$ is treated in a similar way

$$\int_{t^f}^{t^{f+1}} \int_{CV_i} (Q_{per\,m}(T) + Q_{met\,m}(T)) \mathrm{d}V\mathrm{d}t$$
$$\cong [(Q_{per})_i^f + (Q_{met})_i^f] \Delta V_i \Delta t$$
$$= [c_b (G_{b3})_i^f (T_b - T_i^f) + (Q_{met})_i^f] \Delta V_i \Delta t. \qquad (13)$$

The term determining heat conduction between $CV_i$ and its neighbourhoods $CV_{i(j)}$ can be written (for the explicit scheme) in the form

$$\int_{t^f}^{t^{f+1}} \int_{A_i} \mathbf{n} \cdot [\lambda_m(T) \nabla T_m(r,z,t)] \mathrm{d}A \mathrm{d}t$$

$$= \int_{t^f}^{t^{f+1}} \left( \sum_{j=1}^{n_i} \int_{A_{i(j)}} \mathbf{n}_{i(j)} \cdot [\lambda(T) \nabla T(r,z,t)]_{i(j)} \mathrm{d}A_{i(j)} \right) \mathrm{d}t$$

$$\cong \int_{t^f}^{t^{f+1}} \left( \sum_{j=1}^{n_i} \mathbf{n}_{i(j)} \cdot [\lambda(T) \nabla T(r,z,t)]_{i(j)} A_{i(j)} \right) \mathrm{d}t$$

$$\cong \Delta t \sum_{j=1}^{n_i} \mathbf{n}_{i(j)} \cdot [\lambda(T) \nabla T(r,z,t)]_{i(j)}^f A_{i(j)} = \Delta t \sum_{j=1}^{n_i} \Phi_{i(j)}^f A_{i(j)}. \tag{14}$$

In the case when $A_{i(j)}$ is placed between $CV_i$ and internal $CV_{i(j)}$ then $\Phi_{i(j)}^f$ is approximated as follows

$$\Phi_{i(j)}^f = \mathbf{n}_{i(j)} \cdot [\lambda_m(T) \nabla T(r,z,t)]_{i(j)}^f$$

$$= \lambda_{ij}^f \frac{T_{i(j)}^f - T_i^f}{h_{i(j)}} = \frac{T_{i(j)}^f - T_i^f}{R_{i(j)}^f} \tag{15}$$

where $\lambda_{ij}$ is the harmonic mean thermal conductivity between nodes $p_i$ and $p_{i(j)}$ defined as

$$\lambda_{ij}^f = \frac{2\lambda_i^f \lambda_{i(j)}^f}{\lambda_i^f + \lambda_{i(j)}^f} \tag{16}$$

and $R_{i(j)}^f = h_{i(j)} / \lambda_{ij}^f$ is the thermal resistance. If $A_{i(j)}$ is a part of the boundary $\Gamma_{b1}$ or $\Gamma_{b2}$ then one of the boundary conditions (7) or (8) is used and in this case, the following formula is applied

$$\Phi_{i(j)}^f = \frac{T_{amb}(t^f) - T_i^f}{\frac{h_{i(j)}}{2\lambda_i^f} + \frac{1}{\alpha}} \tag{17}$$

where $T_{amb}(t^f) \in \{T_{amb\ air}(t^f), T_{amb\ liq}(t^f)\}$ and $\alpha \in \{\alpha_{air}, \alpha_{liq}\}$ should be selected, respectively. One can see that the denominator in the above formula corresponds to the thermal resistance related to the Robin boundary condition. If $A_{i(j)}$ is a part of the boundary $\Gamma_0$ or $\Gamma_z$ then the Dirichlet boundary condition (6) is used and the formula determining $\Phi_{i(j)}^f$ is of the form

$$\Phi_{i(j)}^f = \frac{T_{tissue} - T_i^f}{\frac{h_{i(j)}}{2\lambda_i^f}}. \tag{18}$$

In the case when $A_{i(j)}$ coincides with the axis $r = 0$ then

$$\Phi_{i(j)}^f = 0 \text{ or equivalent, i.e., } \Phi_{i(j)}^f = \frac{T_{tissue} - T_i^f}{\infty}. \tag{19}$$

At the stage of numerical computations, in the place of $\infty$ a large value, i.e., $10^{10}$ can be assigned.

In order to ensure the unification of notations of the boundary formulas (17), (18) and (19) with the general formula (15), one can use the following values

$$T_{i(j)}^f \in \{T_{amb\ air}(t^f), T_{amb\ liq}(t^f), T_{tissue}, T_{tissue}\} \text{ and}$$

$$R_{i(j)}^f \in \left\{ \frac{h_{i(j)}}{2\lambda_i^f} + \frac{1}{\alpha_{air}}, \frac{h_{i(j)}}{2\lambda_i^f} + \frac{1}{\alpha_{liq}}, \frac{h_{i(j)}}{2\lambda_i^f}, \infty \right\} \tag{20}$$

dependent on the appropriate boundary conditions.

The energy balance (11) written in the explicit form leads to the equation

$$c_i^f (T_i^{f+1} - T_i^f) \Delta V_i = \Delta t \sum_{j=1}^{n_i} \Phi_{i(j)}^f A_{i(j)}$$

$$+ [c_b (G_{b3})_i^f (T_b - T_i^f) + (Q_{met})_i^f] \Delta V_i \Delta t \tag{21}$$

or

$$T_i^{f+1} = T_i^f + \frac{\Delta t}{c_i^f} \left[ \frac{1}{\Delta V_i} \sum_{j=1}^{n_i} \frac{T_{i(j)}^f - T_i^f}{R_{i(j)}^f} A_{i(j)} \right.$$

$$\left. + c_b (G_{b3})_i^f (T_b - T_i^f) + (Q_{met})_i^f \right]. \tag{22}$$

The initial condition (4) is implemented as $T_i^0 = T_{init}$, $i = 1, ..., N$.

In order to ensure the stability condition of explicit scheme (22) the coefficient related with $T_i^f$ must be positive

$$1 - \frac{\Delta t}{c_i^f} \left[ \frac{1}{\Delta V_i} \sum_{j=1}^{n_i} \frac{A_{i(j)}}{R_{i(j)}^f} + c_b (G_{b3})_i^f \right] > 0 \tag{23}$$

for all control volumes $CV_i$, $i = 1, \ldots, N$. Hence, it allows one to determine the critical time step $\Delta t$

$$\Delta t < \frac{c_i^f}{\frac{1}{\Delta V_i} \sum_{j=1}^{n_i} \frac{A_{i(j)}}{R_{i(j)}^f} + c_b (G_{b3})_i^f}. \tag{24}$$

# 3. Results

Two numerical simulations of thermal processes proceeding in the tooth domain have been executed. In Fig. 2, the shape and dimensions of the domain considered and the control volume mesh are presented.

The following thermophysical parameters of the tooth layers have been assumed [9]: $c_1 = 750$, $c_2 = 1170$, $c_3 = 4200$ J/(kg K), $\rho_1 = 2900$, $\rho_2 = 2100$, $\rho_3 = 1000$ kg/m$^3$, $\lambda_1 = 0.92$, $\lambda_2 = 0.63$, $\lambda_3 = 0.59$ W/(m K). The initial temperature is $T_{init} = 36.6$ °C, the temperature of the ambient fluid is $T_{liq\ amb}(t) = -50 + 5\cdot(t - t_1)$ °C and the heat transfer coefficient is $\alpha_{liq} = 1000$ W/(m$^2$ °C), while parameters for the air are the following $T_{air\ amb}(t) = 25$ °C and $\alpha_{air} = 25$ W/(m$^2$ °C). In simulations two contact times $t_{contact} = 2$ s and $t_{contact} = 4$ s, the time limits $t_1 = 60$ s, $t_2 = 90$ s and the tissue temperature $T_{tissue} = 36.6$ °C have been assumed.

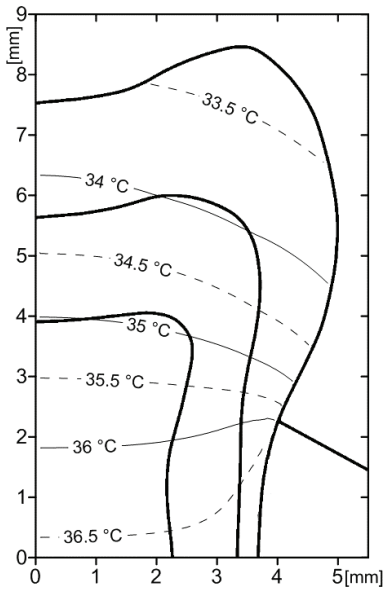


Fig. 4. Temperature distribution in the tooth sub-domains at time 60 s

In Figs. 4, 5 and 6, the isotherms in the tooth sub-domains for times 60 s, 60 s + $t_{contact}$, and 75 s are shown, respectively. The kinetics of temperature variation at selected points A, B and C located near the boundaries of tooth sub-domains (see Fig. 2) are presented in Fig. 7. Figure 8 shows the time derivatives of temperature at points B and C. The control volumes represented by the central nodes B and C are placed in the dentin and the pulp sub-domains, respectively.

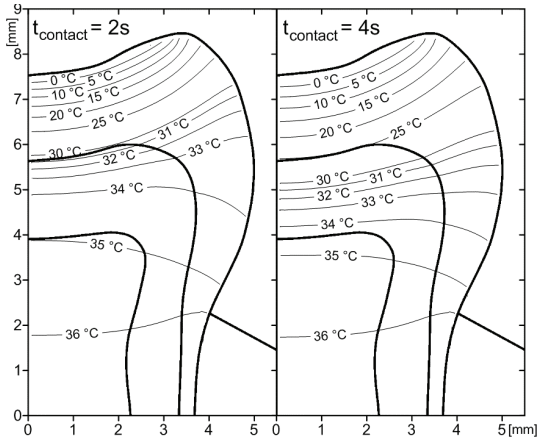


Fig. 5. Temperature distribution in the tooth sub-domains at time 60 + $t_{contact}$ [s]

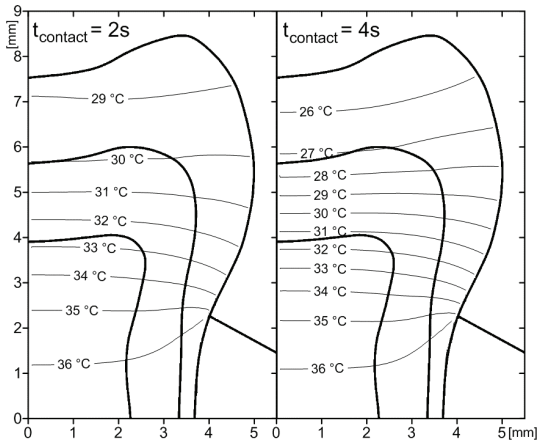


Fig. 6. Temperature distribution in the tooth sub-domains at time 75 s

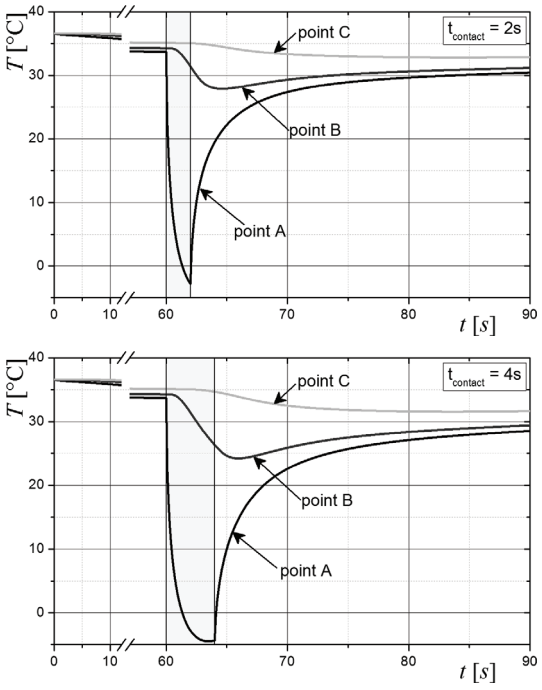


Fig. 7. The kinetics of temperature variation at selected points (see Fig. 2)

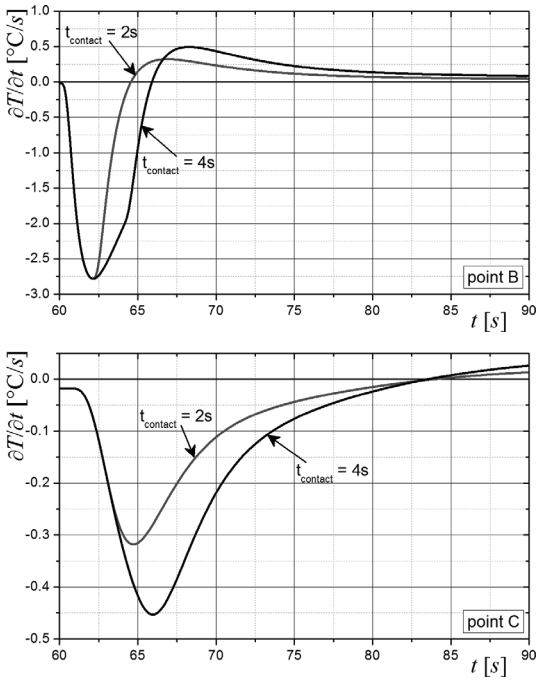


Fig. 8. The time derivatives at points B and C (see Fig. 2)

# 4. Discussion

First of all, the authors assumed that the temperature of the tooth at the initial moment of time corresponds to the average body temperature (36.6 °C). Next, for 1 minute the patient has his mouth open, while the dentist prepares to perform a diagnostic test. At this time, the tooth is cooled by the process of breathing (periodic breathing out of cool air and warm air exhalation). At the stage of numerical modeling the certain simplification is introduced, namely a constant average temperature in the oral cavity for a period of 1 minute is assumed. The amount of heat dissipated by the tooth at this time depends on, among others, the frequency and intensity of breathing, the geometry of the mouth, the ambient temperature and ambient humidity, etc. It is a complex process, and the heat exchange at the stage of calculations was essentially simplified by the assumption of the constant heat transfer coefficient occurring in the Robin boundary condition. On the basis of the temperature field shown in Fig. 4 one can see that, as a result of cooling, the maximum temperature drop on the crown surface equals about 3 K. The temperature field in Fig. 4 corresponds to the state where a rapid cooling of the tooth (under the influence of an external factor) begins. The problem of rapid cooling in the modeled task has also been simplified by the use of the third kind of boundary condition (the Robin condition) and the adoption of the surrounding medium temperature in the form of functional dependence, while the heat transfer coefficient is assumed to be a constant value. The course of the function $T_{liq\ amb}(t)$ depends on many factors, but it should be an increasing function because the soaked swab (the moistened cotton pellet) is heated by the warmer tooth in the mouth.

Figures 5 and 6 show the temperature fields obtained for different contact times between the coolant and tooth, while in Fig. 7 the temperature histories at selected points are presented. It can be seen that the temperature differences on the crown surface in the period of two analyzed contact times during rapid cooling are small. In contrast, the differences are more noticeable in the inner layers of the tooth – especially in the areas close to the boundary between the enamel and dentin (point B). Analyzing the kinetics of temperature changes, one can conclude that the reduction of temperature inside the tooth takes place even after the tooth contact with a cotton swab. The temperature drop in the dentin layer at point B (see Fig. 8) is noticeable even a few seconds after the direct liquid cooling and the maximum value reaches almost 3 K/s. In the pulp layer at point C, the temperature drop is smaller (up to 0.5 K/s) and takes a long period of time. The rapid drop in temperature in the dentin layer causes a change in pressure of the dentinal fluid within the channels and its contraction (according to one theory of pain sensation), so that movement of the fluid can cause irritation of the nerve fibers. In the damaged (dead) tooth there are no active nerve fibers and the pain should not be felt.

So far, we did not find any similar results (from both experimental and mathematical models) in the literature that can be used to analyse and compare with our numerical simulation results. From an experimental point of view, the use of the vital tooth (in the in vivo investigation) is rather impossible for ethical reasons. The widely used method to study the thermal behaviour of human tooth in vitro is based on thermocouples, but it can be technically challenging to the study due to the small size and complex geometrical structure of the biological tooth. These experimental results may contain measurement errors and their cause is, e.g., low spatial resolution and contact measurement. For a vital tooth, the subgingival part of the tooth is surrounded by the environmental tissues with blood vessels.

Several works were related to the experiments with teeth. In work [20], the replica of an axisymmetric model of tooth for experimental purposes has been used in order to simulate the thermal processes occurring while drinking hot liquids. Jakubinek et al. [9]

have been modelled and simulated the process of photopolymerization and related to it the changes in temperature during light-curing of dental restorations. In paper [11], the authors presented the experimental results (also in vitro) as the field temperature distribution on the surface of a cross-section of a human molar tooth, sliced longitudinally into two halves. The tooth was heated by circulating hot water and cooled down by air, and at the same time the infrared camera registered the tooth surface temperature. One can notice that such experimental approaches (the research carried out in the laboratories) do not fully correspond with the biological reality. The main aim of experimental studies, first of all, was to determine the thermophysical parameters of particular layers of a tooth and the parameters of conditions acting on the tooth, which can be used in simulations performed on the basis of mathematical models. It should be mentioned that the way of modelling of the heat transfer problem proceeding during pulp vitality testing so far has not appeared in the known works.

# 5. Conclusions

A very common problem discussed in academic works is tooth sensitivity to various external stimulations. The model presented can provide information related to the temperature field in the tooth and the kinetics of the temperature changes in the various tooth sub-domains and the simulation results can assist dentists in the selection of an appropriate method of diagnostics and treatment. For example, directly after the completion of freezing the temperature at point A increases, while at points B and C it continues to decrease. This results from the reduced temperature of the enamel sub-domain. So, the cooling effect lasts longer than the thermal contact with the coolant. In other words, a sudden drop of temperature at points placing in pulp and dentin sub-domains can cause sharp pain in the tooth, lasting even a few seconds after completion of freezing.

The results of numerical simulations discussed here concern the selected tooth geometry, but the algorithm presented can be used for the different parameters occurring in the mathematical model and any geometrical shape of the tooth.

In this paper, the possibilities of the CVM application for a numerical solution of the bioheat transfer are shown. The control volume meshes (using the Voronoi polygons) accurately reproduce the geometry of the tooth (if the assumption that 2D axially-symmetrical approximation is acceptable) – it is an essential advantage of the method proposed.

In the future, research is planned connected with the elaboration of the numerical algorithm based on the control volume method in which the thermophysical parameters of tooth sub-domains will be treated as the interval numbers [15], [17]. This results from the fact that the biological tissue properties are dependent on the individual characteristics such as gender, age etc. Additionally, the experimental research using the thermal imaging techniques will be realized. Such a study will allow one (at least) to observe the course of transient temperature field on the surface of the tooth crown.

# References

[1] CHEN E., ABBOTT P.V., *Dental Pulp Testing: A Review*, Int. J. Dent., 2009, 365785.

[2] CHONG B.S., *Harty's Endodontics in Clinical Practice*, 6th ed., Churchill Livingstone, 2010.

[3] CIESIELSKI M., MOCHNACKI B., *Application of the Control Volume Method using the Voronoi polygons for numerical modeling of bio-heat transfer processes*, J. Theoret. Appl. Mech., 2014, Vol. 52(4), 927–935.

[4] CIESIELSKI M., MOCHNACKI B., *Numerical simulation of the heating process in the domain of tissue insulated by protective clothing*, J. Appl. Math. Comput. Mech., 2014, Vol. 13(2), 13–20.

[5] DE VREE J.H.P., SPIERINGS TH.A.M., PLASSCHAERT A.J.M., *A Simulation Model for Transient Thermal Analysis of Restored Teeth*, J. Dent. Res., 1983, Vol. 62, 756–759.

[6] DOMANSKI Z., CIESIELSKI M., MOCHNACKI B., *Application of Control Volume Method using the Voronoi Tessellation in Numerical Modelling of Solidification Process*, [in:] A. Korsunsky (ed.), Current Themes in Engineering Science 2009, AIP Conf. Proc., 2010, Vol. 1220, 17–26.

[7] GOPIKRISHNA V., PRADEEP G., VENKATESHBABU N., *Assessment of pulp vitality: a review*, Int. J. Paediat. Dent., 2009, Vol. 19(1), 3–15.

[8] JAFARZADEH H., ABBOTT P.V., *Review of pulp sensibility tests*. Part I: *General information and thermal tests*, Int. Endod. J., 2010, Vol. 43, 738–762.

[9] JAKUBINEK M.B., O'NEILL C., FELIX C., PRICE R.B., WHITE M.A., *Temperature excursions at the pulp-dentin junction during the curing of light-activated dental restorations*, Dent. Mater., 2008, Vol. 24, 1468–1476.

[10] LIN M., XU F., LU T.J., BAI B.F., *A review of heat transfer in human tooth – Experimental characterization and mathematical modeling*, Dent. Mater., 2010, Vol. 26, 501–513.

[11] LIN M., LIU Q.D., XU F., BAI B.F., LU T.J., *In vitro investigation of heat transfer in human tooth*, 4th Int. Conf. Adv. Exp. Mech. (18–20.11.2009), Singapore, 2009.

[12] MAJCHRZAK E., *Application of different variants of the BEM in numerical modeling of bioheat transfer problems*, Mol. Cell. Biomech., 2013, Vol. 10(3), 201–232.

[13] MAJCHRZAK E., MOCHNACKI B., DZIEWOŃSKI M., JASIŃSKI M., *Numerical modeling of hyperthermia and hypothermia proc-*

*esses*, Computational Materials Science, PTS 1-3. Book Series: Adv. Mater. Res, 2011, Vol. 268–270, 257–262.

[14] MOCHNACKI B., MAJCHRZAK E., *Sensitivity of the skin tissue on the activity of external heat sources*, Comp. Model. Eng. Sci., 2003, Vol. 4(3–4), 431–438.

[15] MOCHNACKI B., PIASECKA BELKHAYAT A., *Numerical modeling of skin tissue heating using the interval finite difference method*, Mol. Cell. Biomech., 2013, Vol. 10(3), 233–244.

[16] OKABE A., BOOTS B., SUGIHARA K., CHIU S.N., *Spatial Tessellations: Concepts and Applications of Voronoi Diagrams*, 2nd ed., Wiley, 2000.

[17] PIASECKA BELKHAYAT A., *Interval boundary element method for 2D transient diffusion problem using the directed interval arithmetic*, Eng. Anal. Bound. Elem., 2011, Vol. 35(3), 259–263.

[18] PREISKORN M., ŻMUDA S., TRYKOWSKI J., PANAS A., PREISKORN M., *In vitro investigations of the heat transfer phenomena in human tooth*, Acta Bioeng. Biomech., 2003, Vol. 5(2), 23–36.

[19] SIEDLECKI J., CIESIELSKI M., *Simulations of thermal processes in a restored tooth*, J. Appl. Math. Comput. Mech., 2013, Vol. 12(4), 103–108.

[20] SPIERINGS T.A., PETERS M.C., BOSMAN F., PLASSCHAERT A.J., *Verification of theoretical modeling of heat transmission in teeth by in vivo experiments*, J. Dent. Res., 1987, Vol. 66(8), 1336–1339.